MACHINABILITY AND PROCESS STABILITY WHEN TURNING ALLOY 718 WITH STANDARD AND PRODUCED BY SELECTIVE LASER SINTERING TOOLHOLDERS

O. A. Gutnichenko[1], V. M. Bushlya[1], J. M. Zhou[1], J.-E. Ståhl[1], P. Avdovic[2], U. Simmons[2]

[1] Division of Production and Materials Engineering, Lund University, Ole Römers väg 1, 22100 Lund, Sweden
[2] Siemens Industrial Turbomachinery AB, 61283 Finspång, Sweden

Email of communication author: *Oleksandr.Gutnichenko@iprod.lth.se*

The paper presents the results of a comparative analysis of machinability and dynamic stability when turning a nickel-based superalloy with whisker reinforced alumina (WRA) tools in a conventional and prototype toolholders. The use of the prototype toolholder with a spatial structure is shown to significantly suppress vibrations during the machining and stabilize the process within the cutting speed range between 200 and 400 m/min. The above mentioned benefits are demonstrated to be owing to damping properties of the proposed toolholder.

Keywords Alloy 718, turning, machinability, tool wear, surface quality, dynamic stability, wavelet transform, 0-1 test

1. INTRODUCTION

Nickel based superalloys are widely accepted by airspace and other industries for the manufacture of jet engines, gas turbines, etc. The attention focused on this class of heatresistant alloys is due to their capability of high mechanical properties to be retained under extreme operating conditions. The most known material in this class – age hardened Inconel 718 – shows a high strength and corrosion resistance at temperatures up to 650°C. These properties offer this alloy a wide range of applications but, at the same time, make it a difficult to machine material (Arunachalam R.et al., 2000).

The ordinary used tool materials for machining Inconel 718 are coated carbides, ceramics, and materials based on cubic boron nitride (cBN). In high-speed operations the ceramic and cBN tools hold greater promise and offer a number of benefits for improving efficiency of material machining (Arunachalam R.M. et al., 2004). As demonstrated in (Zhou, J.M. et al., 2011, 2012), in turning Inconel 718 with SiC whisker reinforced alumina (WRA) tools in a wide range of cutting speeds, the dependency of the integrity of the machined surface and subsurface layer on the tool wear exhibits a complex trend. With the tool wear increasing almost linearly, the quality of the workpiece surface deteriorates significantly throughout the machining process. According to (Zhou, J.M.et al., 2012), the main factors responsible for surface defects are the fracture of TiC/NbC carbides in the course of cutting and the specifics of surface generation – the plastic flow of the material towards the minor cutting edge. The main wear mechanisms in the tool are the diffusion and abrasion, the latter being dominant. As the cutting speed is increased the mechanical fracture of the tool edge due to a relatively low fracture toughness of WRA occurs (Nakao, W. et al., 2005, Kumar, A.S. et al., 2006). The development of tool wear results in the generation of self-excited vibrations in the cutting system and leads to the process instability. The latter, in turn, promotes both the tool and machine components damage as well as affects the machined surface finish.

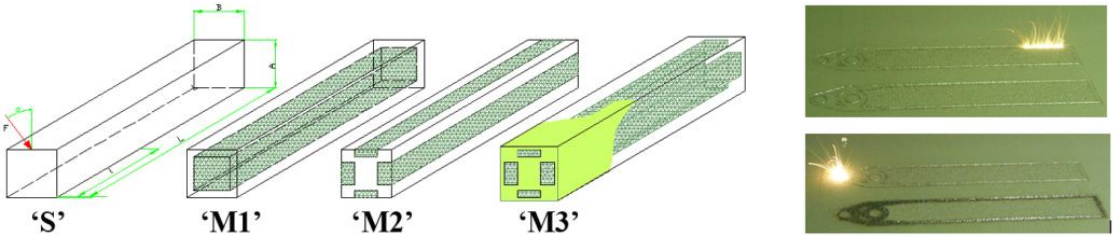

a) b)

Fig. 1. Designs of developed toolholders (a) and procedure of selective laser sintering powder (b).

The problems of abrasive wear and mechanical failure of tools are conventionally resolved by using advanced materials based on polycrystalline cBN (Bushlya, V. et al., 2012). Another widely accepted approach for reducing the extent of impact actions on the tool is using active dampers or passive damping hybrid structures (Parka, G. et al., 2007). Siemens Industrial Turbomachinery AB (Sweden), a manufacturer of gas and steam turbines, has proposed new method for solving this problem. The company has designed a toolholder with a cellular spatial structure (see Fig. 2.c) which should provide additional damping properties for the dynamic system. The prototype toolholder was manufactured by the selective laser sintering of powders. The experimental designs of developed toolholders and sintering procedure are shown in Fig. 1. The present work addresses a comparative analysis of benefits of machinability of Alloy 718 and process stability when turning the alloy with an WRA tool using a conventional toolholder (CH) and a laser sintered toolholder (LSH) over a wide range of cutting speed (v_c = 100-500 m/min).The process dynamics was analyzed on the basis of results of processing spectra of cutting forces and tool accelerations through calculation of signal characteristics in time and frequency domains. The process stability was assessed by the analysis of tool tip trajectories.

2. MATERIALS, TECHNIQUES AND TEST SETUP

Machining tests were run on a 70 mm diameter and 210 mm long bar workpiece of Alloy 718 supplied in solution annealed and aged (precipitation hardened) conditions (HRC, 45±1). WRA inserts with geometry RNGN 120700T01020 (12.7 mm in diameter, 7.94 mm thick) were used as the tool material. The inserts were honed with the edge radius of 25 to 28 μm, the chamfer was 0.1×20°. The CH toolholder and LSH toolholder with design 'M1' had the same geometry (CRDNN 3225P12-ID (ISO)) as shown in Fig. 2; the tool back rake angle was -6°.

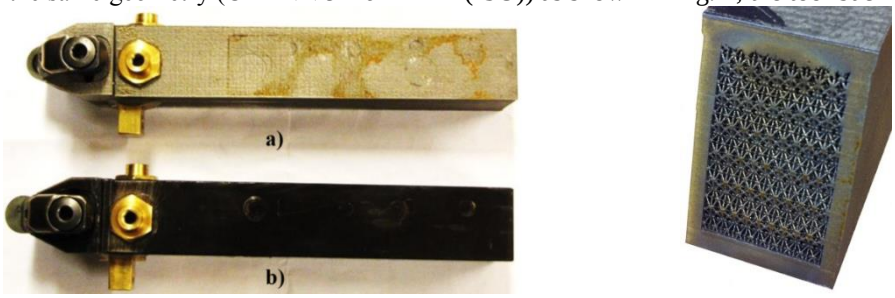

c)

Fig. 2. General view of tested toolholders: a) designed by the selective laser sintering; b) standard tool; c) designed internal structure of experimental tool.

The longitudinal turning was performed on a CNC lathe SMT500, using 8% solution of Sitala D201-03 (Shell) fluid as a coolant. The cutting conditions were as follows: cutting speed v_c = 100, 200, 300, 400, and 500 m/min; feed rate f = 0.1 and 0.2 m/min; depth of cut was constant, a_p = 0.3 mm.

To compare the machinability and cutting process dynamics for both standard and laser sintered toolholders, we studied the force and acceleration spectra, machined surface parameters, and tool wear characteristics. The cutting forces were measured using a Kistler 9129AA three-axis piezoelectric dynamometer. Vibrations were monitored by means of Bruel & Kjaer 8309 piezoelectric accelerometers placed along three mutually perpendicular directions. Spectra of cutting forces and accelerations were recorded simultaneously with sampling rates of 1 and 120 kHz, respectively. Processing of the spectra was performed using LabView and Matlab software packages, by conventional as well as advanced signal processing methods. The process dynamic stability was studied by 0-1 test. The tool flank wear (VB) was measured on Leica MZ16 stereomicroscope. The tool wear morphology was examined by scanning electron microscopy (LEO SEM 1560) and optical 3-D microscope Alicona Infinite Focus.

3. RESULTS AND DISCUSSION

3.1. Assessment of damping and stiffness properties of CH and LSH tools

The capability of toolholders to suppress free vibrations was estimated by the study of pulse response of dynamic system to an impact load. The impact load was made by the impact pendulum-type testing machine with energy E ≈ 40 J. The vibration spectra for both toolholders are presented in Fig. 3.a. A logarithmic decrement was considered as a characteristic of system's damping capacity and was calculated by the next expression:

$$\delta = \frac{\sum \ln\left(\frac{A_i}{A_{i+1}}\right)}{n-1},$$

where A_i – maxima values on the response curves, $i = 1 \ldots n$.

The calculated values of decrements were equal $\delta_{CH} = 0.07375$ and $\delta_{LSH} = 0.2449$ for CH and LSH toolholders, respectively. The amplitude of acceleration signal for standard toolholder, by the way, has a difference in 2 orders as compared to laser sintered one. The estimation of the stiffness of the considered toolholders was performed by the determination of their natural frequencies. The normalized power spectra of the obtained responses are shown in Fig. 3.b. It is easy to determine that the mentioned frequencies are 1953 Hz and 1342 Hz for CH and LSH toolholders, respectively. Taking into account that the relative stiffness $k = c/m = \omega_0^2$ is proportional to a squared natural frequency ω_0, the ratio of the stiffness coefficients is $k_{CH} : k_{LSH} \approx 2:1$.

Further work in the article is addressed the study of a question how that difference in toolholders' structural properties influences on the machinability and dynamic stability of cutting process.

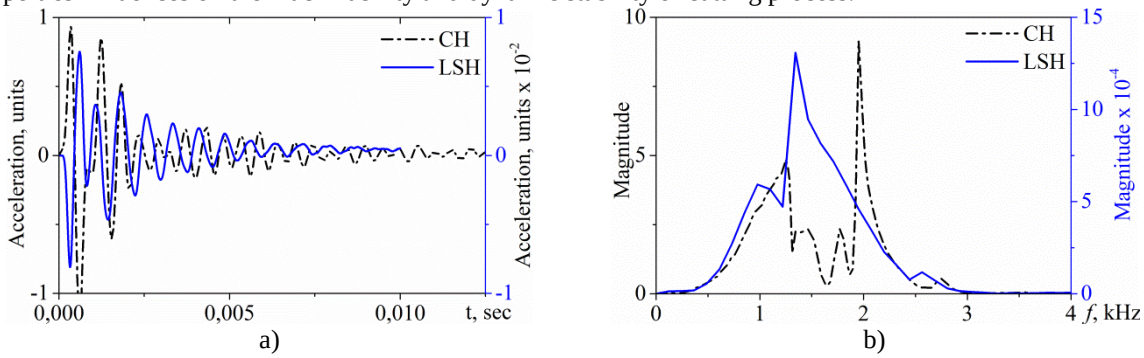

Fig. 3. Pulse response characteristics of toolholders: a) acceleration signals; b) normalized power spectra.

3.2. Machinability of Alloy 718

Cutting forces and their development during the tool wear

Table 1. Cutting forces and average values of accelerations.

v_p, m/min	f, mm/rev	Cutting forces F_{CH}/F_{LSH}, N, for fresh tool			Cutting forces F_{CH}/F_{LSH}, N, for worn tool			Average values of acceleration amplitudes (a_{CH}/a_{LSH}), rel. units		
		z	*y*	*x*	*z*	*y*	*x*	*z*	*y*	*x*
100		210/200	270/250	100/90	400/380	800/734	300/370	0,5/0,2	0,3/0,3	0,2/0,1
200		232/240	280/300	120/120	440/425	1140/1070	440/400	1,5/0,7	0,8/0,3	0,5/0,2
300	0,1	166/170	190/220	80/90	370/425	1315/1370	440/480	2,2/0,9	1,0/0,5	0,6/0,3
400		180/200	225/255	90/110	350/400	1090/1150	360/440	2,2/0,7	1,0/0,4	1,1/0,3
500		175/160	205/260	90/110	345/350	1000/1130	360/410	3,4/0,6	1,5/0,4	0,8/0,3
100		380/340	380/350	150/130	515/500	715/610	285/240	0,6/0,5	0,7/0,2	0,4/0,6
200		350/285	324/270	130/100	485/435	880/750	340/290	2,3/1,5	1,5/0,5	0,8/0,4
300	0,2	360/348	380/410	125/130	485/505	770/780	300/315	4,4/1,3	1,8/0,7	1,4/0,3
400		278/300	240/250	100/100	410/420	780/800	280/300	6,0/1,3	2,5/0,5	2,0/0,7
500		332/270	270/310	235/220	445/400	1110/1020	370/340	8,5/1,6	5,2/0,8	2,6/0,7

Note: F_{CH}, a_{CH} and F_{LSH}, a_{LSH} are forces and average values of acceleration amplitudes in turning with CH and LSH tools, respectively.

The data on cutting forces observed in turning Inconel 718 with CH and LSH tools in the fresh and worn states (cutting length L = 210 m) are summarized in the table 1.

In the course of cutting the forces grow mostly in a linear manner (see the table), except for the cases where flaking on the rake face of the insert was observed. A comparative analysis of the test results obtained under various machining conditions has revealed the following.

1. Feed rate f = 0.1 mm/rev. The coefficient $\alpha_F = F_{CH}/F_{LSH}$ is about 1.0 over the entire cutting speed range for both tool types. As the tool wear increases the values of the tangential cutting force component is doubled, the axial one increases up to 3 to 4 times, and the radial component increases 5-fold in comparison to the fresh tool. Approximately the same situation occurs at conditions when feed rate f = 0.2 mm/rev and fresh tool except the low cutting speeds where the coefficient $\alpha_F(v_c)$ increases to 1.2–1.3.
2. Feed rate f = 0.2 mm/rev, worn tool. The trend of the functions $\alpha_F(v_c)$ is identical to that in the previous case, but absolute values of the tangential and axial force components increase 1.5-fold and that of the radial component by a factor of 4–5 in comparison to the fresh tool (see the Table 1), which is typical for round inserts.
A comparison between various machining conditions shows that as the feed rate for a fresh tool is raised the values of the cutting force increase 1.5–2.0 times, while for the worn tools the difference is insignificant and decreases with increasing cutting speed.
A different situation is with acceleration spectra. As evident from the Table 1, $a_{CH}/a_{LSH}(v_c)$ grows for all acceleration components and varies between 1 and 6 with increasing cutting speed, irrespective of the feed rate.
Thus, it has been found that the cutting forces in turning with the conventional tool and the prototype one differ by approximately 25% (max) under the present test conditions. On the other hand, the vibration amplitude in turning with the CH tool is 5–6 times higher than that of the LSH tool. This points to a significant decrease in the vibration level in machining with the sintered toolholder. Suppression of vibrations owing to "improved" damping properties of the proposed toolholder can be judged if the extent and mechanisms of cutting tool wear are similar for both toolholder types.

Tool wear mechanisms and achievable tool life
Figure 4 shows the results of electron microscopy of worn tools under various cutting conditions. Analysis of the results enables us to make some conclusions and comments. It is seen from Fig. 4 that the cutting edge wear mechanism and pattern are similar for both tool types. In both cases, one can observe a crater on the insert face and a uniform flank land. Cutting speed has a significant effect on the tool wear value and the type of damage – rounding of the cutting edge becomes more intensive in the region h_{1min}, the insert face undergo some chipping, which is especially the case with the use of the conventional toolholder. An increase of the cutting speed up to 500 m/min is accompanied by considerable damage of the insert: chipping of the edge, flaking and cracking on the face.

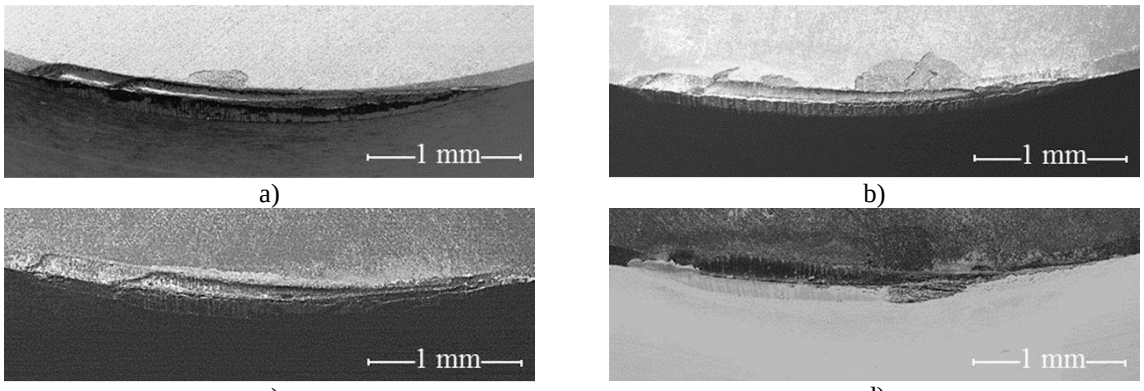

Fig. 4. SEM observation of worn tools at different cutting conditions: a) CH, v_c = 200 m/min, f = 0.1 mm/rev; b) v_c = 400 m/min, f = 0.2 mm/rev; c) LSH, v_c = 200 m/min, f = 0.1 mm/rev; d) v_c = 400 m/min, f = 0.2 mm/rev.

For more obvious understanding tool wear morphology and mechanism as well as proving the mentioned conclusions the data of 3-D microscopy were obtained and are presented in Fig. 5.

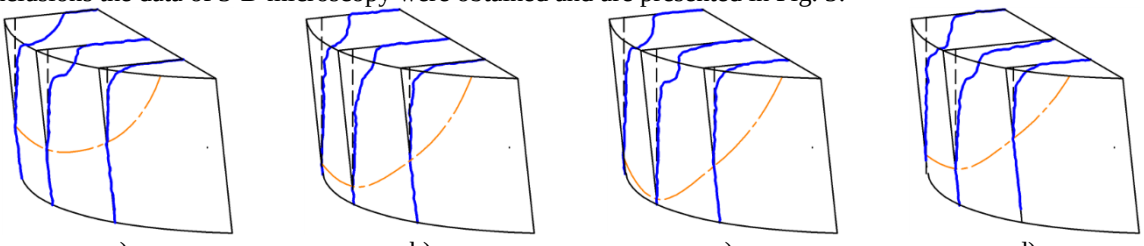

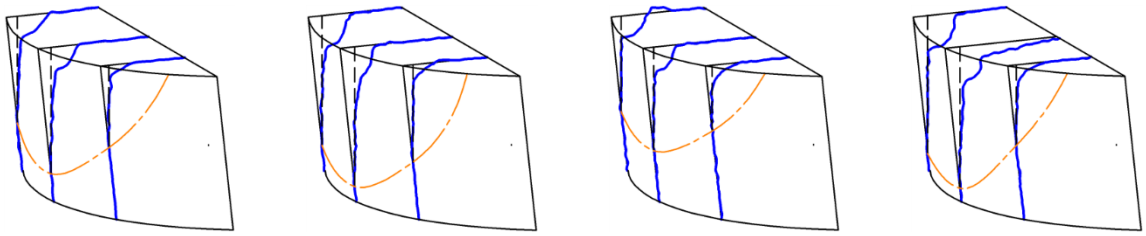

Fig. 5. 3-D observation of worn tools at different cutting speeds and feed rate f = 0.1 mm/rev: CH a) v_c = 100 m/min; b) v_c = 200 m/min; c) v_c = 300 m/min; d) v_c = 400 m/min; LSH e) v_c = 100 m/min; f) v_c = 200 m/min; g) v_c = 300 m/min; h) v_c = 400 m/min.

The profiles in the Fig. 5 and 6 are measured at the cross-sections of maximum chip thickness, middle of cutting edge and in the vicinity of h_{1min}, respectively. It is seen that increase of cutting speed from 100 to 400 m/min is accompanied by increase of crater size on the rake face and flank wear land. It should be noted that CH tools are more predisposed to appearance of negative clearance angle at cutting speed range higher 200 m/min at low feed rate f = 0.1 mm/rev than LSH ones which have obviously negative clearance angle at 200 m/min. The increase of feed rate value to f = 0.2 mm/rev reduces the difference between two worn tools but the formation of deeper craters and larger flank wear lands occurs as compared to low feed rate case. The negative clearance angle can be observed on CH tools at cutting speeds 200-300 m/min (Fig. 6.b, c) and at 200 m/min (Fig. 6.f) in case of LSH tools what might affect the dynamic stability of cutting process.

The tool performance was assessed by the wear rate defined as a ratio of the flank wear land VB_{max} to the cutting length L: $WR = VB_{max}/L$. The results of the measurements are given in Fig. 7.

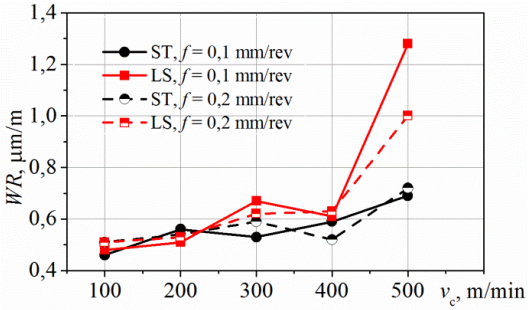

Fig. 7. Specific wear rate at different cutting conditions: a) *f* = 0.1 mm/rev; b) *f* = 0.2 mm/rev.

The wear intensity WR is in fact equal for both tool types at cutting speeds up to 400 m/min and feed rate of 0.1 mm/rev (see Fig. 7). An increase of the feed rate up to 0.2 mm/rev has almost no effect on the wear intensity in turning with CH tool but causes an 10–17% rise in WR in the case of the LSH tool at these high cutting speeds. Thus, in the cutting speed range between 100 and 400 m/min at a feed rate f = 0.1 mm/rev the tool wear can be considered equal for both tool types compared. Hence it follows that the mentioned suppression of vibrations occurs not through the tool wear but is provided owing to the properties of the spatial structure of LSH.

Surface roughness and its evolution with tool wear (cutting length)

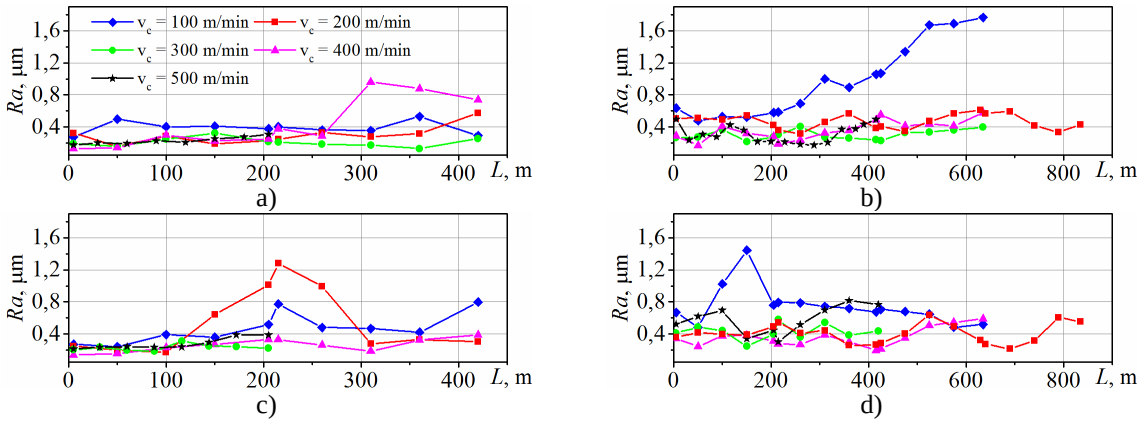

Fig. 8. Surface roughness at different cutting conditions: a) CH tool, *f* = 0.1 mm/rev; b) *f* = 0.2 mm/rev; c) LSH tool, *f* = 0.1 mm/rev; d) *f* = 0.2 mm/rev.

In conclusion of considering the machinability aspects the quality of machined surface was estimated by the measurement of roughness *Ra* depending on different cutting conditions. The corresponding plots are presented in Fig. 8. As demonstrated in the figures the *Ra* values tend to be stable overall the cutting conditions and with development of tool wear and vary in range 0.1-0.6 μm. The highest roughness reaches the value 1.0-1.7 μm at low cutting speeds 100-200 m/min which might correspond to the start of formation of negative clearance angle. In other cases the behavior of roughness dependencies are rather related to chemical and/or friction interactions between tool and workpiece materials.

3.3. Influence of cutting conditions on dynamic stability of process

Spectral and wavelet analyses

In order to estimate the dynamic system response in frequency and time domains the acceleration spectra obtained for the processes at different cutting conditions were undergone Fourier and wavelet transforms. Figure 9 shows the results of FFT analysis for both toolholders depending on cutting conditions. In case of machining with the conventional toolholder at feed rate 0.1 mm/rev the increase of cutting speed causes the increase of vibration amplitudes within low frequency range up to 5 kHz and around 35 kHz. The vibrations with frequency 40-45 kHz appears at speed 200 m/min and remains stable up to 500 m/min. The increase of feed rate to 0.2 mm/rev changes the behavior drastically.

The new harmonics in the frequency ranges 10-18 kHz, 30-40 kHz and 50-60 kHz appear with increase of cutting speed. Such behavior is caused by both the tool vibrations which are related to the development of tool wear and response of machine component on the increase of cutting forces during the cutting process. On the contrary the response of laser sintered toolholder in frequency domain is very weak, especially at low feed rate value, and it is characterized partially by the suppression of vibrations with increase of cutting speed. The main harmonics, in this case, belong to the frequency 7.8 kHz and some activity is present at 30-40 kHz. The increase in feed rate to 0.2 mm/rev causes the intensification of vibrations within the span 25-45 kHz. The given plots allows the considering a general view of the process. More detailed analysis in low frequency range in time-frequency space was performed by the continuous wavelet transform (CWT). The results are presented in Figure 10.

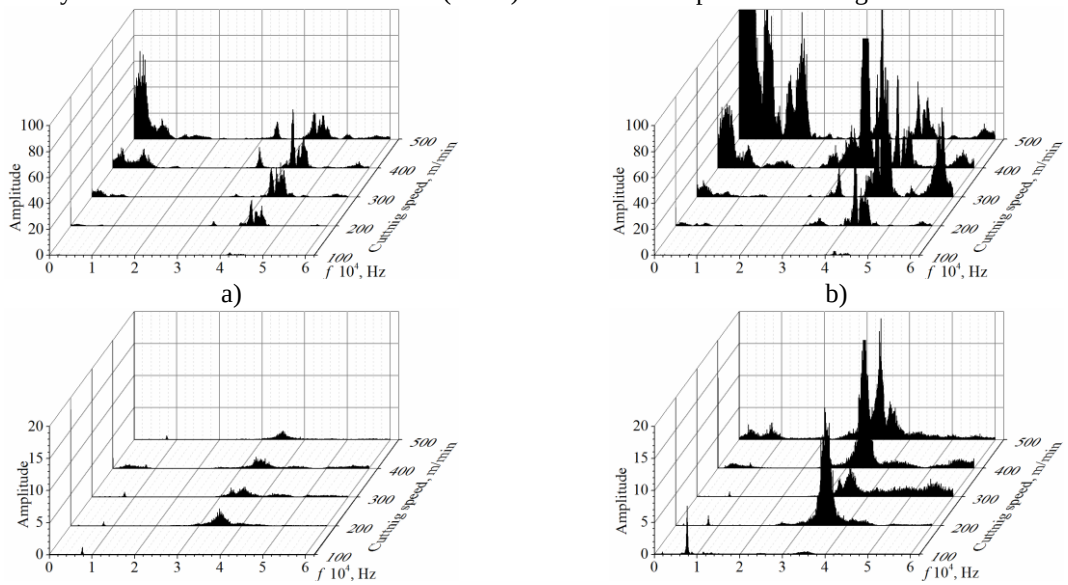

Fig. 9. FFT spectra of acceleration signal in cutting direction depending on cutting conditions: a) CH, f = 0.1 mm/rev; b) f = 0.2 mm/rev; c) LSH, f = 0.1 mm/rev; d) LST, f = 0.2 mm/rev.

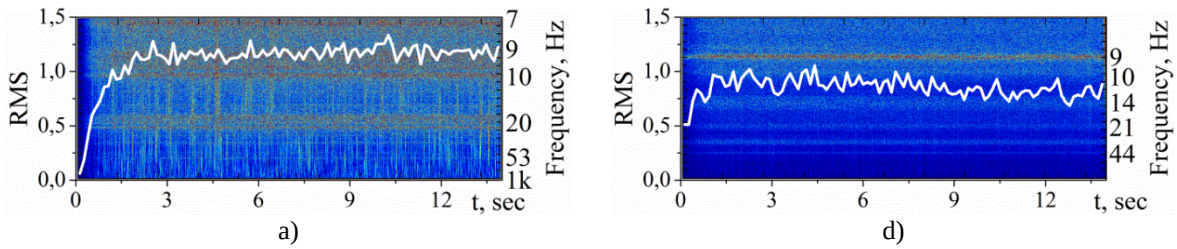

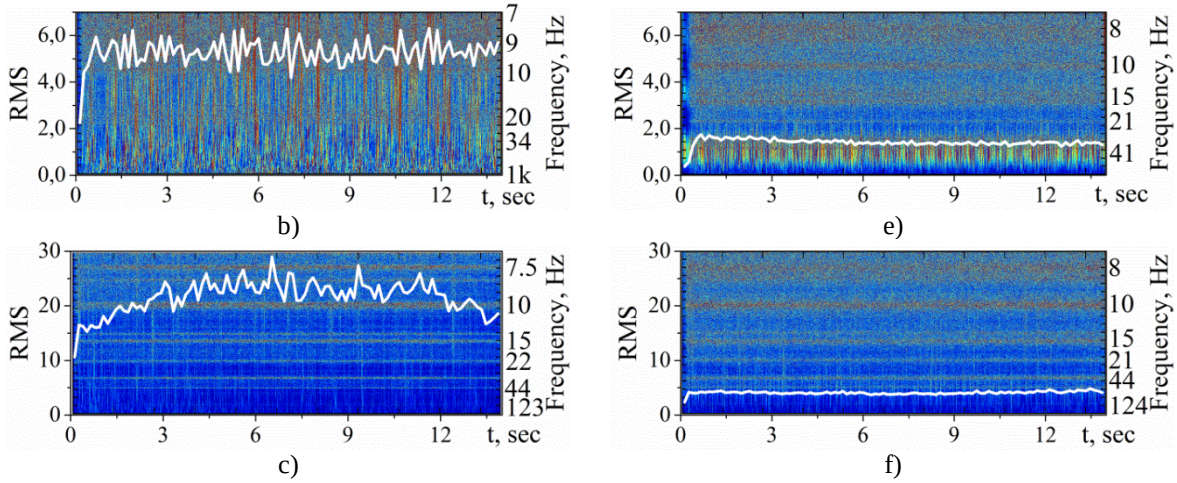

Fig. 10. CWT spectra of vibration signals and dependencies of RMS of wavelet coefficients $C(a, b)_{max}$ (*white curve*) under various cutting conditions (v_c = 100 m/min, f = 0.1 mm/rev (a, d); v_c = 500 m/min, f = 0.1 mm/rev (b, e); v_c = 400 m/min, f = 0.2 mm/rev (c, f)) for CH (a, b, c) and LSH tools (d, e, f).

The acceleration spectra were analyzed using CWT which provides a two-dimensional array of amplitudes (WT coefficients C(a, b)) in the space (a, b) = (frequency, time). For the signal approximation Daubechies wavelet 'db1' was used with a center frequency w_0 = 0.9961 Hz and performed the analysis in the frequency range 6-150 Hz. The time dependence of the maximum CWT coefficients $C(a, b)_{max}$ (white curves in Fig. 11) were used in order to reveal singularities in the acceleration spectra and estimate the noise level.

Based on these findings, the following comments can be made.

1. v_c = 100 m/min. Turning with the LSH tool is characterized by the presence of a stable harmonic with a frequency corresponding to the spindle speed. The tool behavior is actually independent of the feed rate. The wavelet spectrograms for the CH tool show numerous subharmonics and noise over the entire frequency range (see Figs. 10.a, 10.d).
2. v_c = 300-500 m/min, feed rate f = 0.1 mm/rev. In turning with the LSH tool, there arise subharmonics in addition to the main harmonic and a slight growth of the noise level in the low frequency region is observed as the cutting speed is raised. With the cutting speed above 400 m/min, some singularities are seen to arise in the vicinity of the frequency that corresponds to the spindle speed. Turning with the CH tool is accompanied by significant noise and singularities, transient process and signal intermittence arising over the entire frequency range. RMS values of C_{max} are 15 and 6 units at a cutting speed of 400 m/min and 17 and 5.5 units at 500 m/min for the CH and LSH tools, respectively (see Figs. 10.b, 10.e).
3. v_c = 300–500 m/min, feed rate f = 0.2 mm/rev. An increase in the feed rate leads to a significant growth of noise, especially in the case of the conventional toolholder. RMS of C_{max} at a cutting speed of 400 m/min are 50 and 12 for the CH and LSH tools, respectively (see Figs. 10.c, 10.f).

Analysis of tooltip trajectories and 0-1 stability test

Taking into account the low noise level and absence of singularities of vibration signal when machining with LSH tools as compared to conventional one this feature of operation of laser sintered tool has to be reflected in nature of tooltip trajectories. The given vibration signals were denoised and reconstructed in the following way. At first the base noise was subtracted from the obtained FFT spectra of acceleration signals acquired in three orthogonal directions for both toolholders. The *N* highest harmonics of FT which exceeded the threshold of 20% of maximum power with respective phase shift were selected for the signals reconstruction by the expression:

$$f(t) = \sum_{k=1}^{N} A_k \cos(2\pi \cdot f_k + \theta_k).$$

The Poincare (pseudo)maps were chosen in order to estimate and judge about the periodicity and regularity of tool point movements in cutting (*z*), feed (*x*) and passive (*y*) directions. The results of computations are presented in Figure 11.

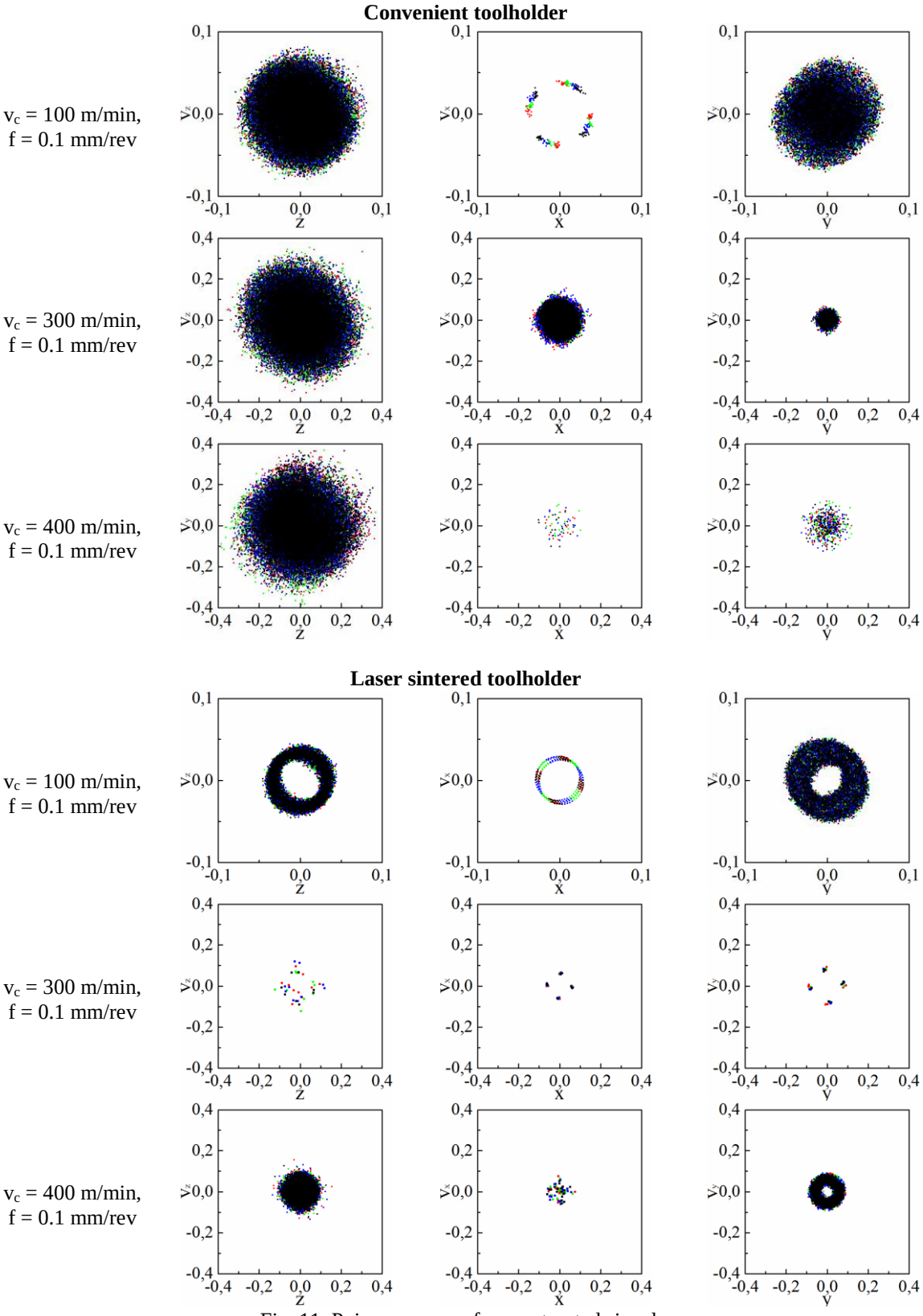

Fig. 11. Poincare maps of reconstructed signals.

The obtained results partially prove the conclusions made above. In accordance with Fig. 11 the conventional toolholder moves aperiodically already when cutting speed increases higher than 200 m/min in all considered direction even at such a strong simplification of signals. The experimental toolholder has regular movements during machining in all directions up to the cutting speeds 300 m/min. The periodic character of tool tip motion can be identified also at higher cutting speeds but only in certain directions. The next question which is considered

is the dynamic stability of tools by the analyses of real signals which consist from reconstructed ones being accompanied with stochastic noise and distortions.
The 0–1 test was applied for the assessment of stability of operation of the tools being compared. Here, the term "stability" implies some regular motion of the system, while a changeover to chaotic behavior denotes a loss of stability. Unlike the definition of Lyapunov exponent, the researchers (Gotwald, G.A. et al., 2009) propose to consider mapping of a time series onto some plane. A special feature of such mapping is that in the case of non-chaotic dynamic of the process the mapping has a periodic or quasiperiodic pattern. The Lyapunov exponent, in turn, represents the rate of divergence of the trajectories in the phase space, i.e., deviation of the dynamic system from its stable motion by the exponential relationship. Thus, a common idea behind the methods can be traced, but the 0–1 test is much simpler for numerical implementation. The results of comparison are given in Fig. 12. The value "1" corresponds to a stable motion and the value "0" to a chaotic motion.

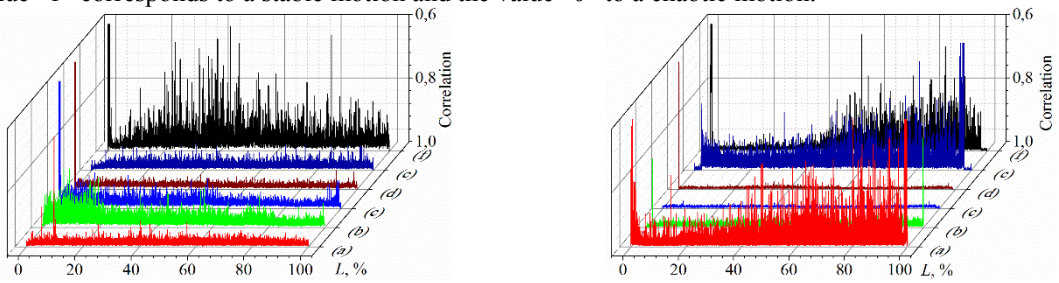

a) b)

Fig. 12. Results of the 0–1 test for (a) CH and (b) LSH tools: 1) v_c = 100 m/min, f = 0.1 mm/rev; 1) v_c = 100 m/min, f = 0.2 mm/rev; 3) v_c = 200 m/min, f = 0.1 mm/rev; 4) v_c = 400 m/min, f = 0.1 mm/rev; 5) v_c = 400 m/min, f = 0.2 mm/rev; 6) v_c = 500 m/min, f = 0.1 mm/rev.

The comparative analysis has demonstrated that as the cutting speed is raised with a feed rate f =0.1 mm/rev the operation of both tools becomes generally stabilized. However, noteworthy are some special features:
– machining with the LSH tool is qualified as unstable at a cutting speed v_c < 200 m/min irrespective of the feed rate (see Figs. 7 a, 7 e);
– the conventional tool is stable at v_c < 200 m/min regardless of the feed rate and loses stability in the cutting speed range between 200 and 300 m/min (see Fig. 6);
– at a feed rate f = 0.2 mm/rev and cutting speeds 200 to 300 m/min the tools work in an unstable manner (see Figs. 6 f and 7 f). As the cutting speed is raised further on (v_c > 300 m/min), the operation of the LSH tool becomes stabilized.

4. CONCLUSIONS

The experimental measurements of cutting speed and acceleration spectra in turning Inconel 718 alloy have demonstrated that the machining with the LSH tool is accompanied by a considerable suppression of vibrations, so that in the case of raising cutting speed up to 500 m/min the vibration amplitude is 5–7 times lower in comparison to the tool in the conventional toolholder. The test conditions and similar wear pattern have enabled us to infer that the suppression of vibrations is owing to damping properties of the honeycomb spatial structure implemented in the prototype toolholder.
The wavelet analysis has revealed that the motion of the LSH tool is characterized by the fundamental harmonic whose frequency corresponds to the spindle speed and by a low noise level over the entire cutting speed range. At high cutting speeds there arise subharmonics and the noise level grows slightly. Analysis of spectral for the CH tool, as opposed to the previous case, has shown a significant (3- to 6-fold) increase of noise and occurrence of singularities in the acceleration spectra at cutting speeds > 200 m/min.
According to the 0–test, the CH tool works in a stable manner at a low cutting speed (v_c = 100 m/min) regardless of the feed rate. At a feed rate f = 0.1 mm/rev a rise of the cutting speed leads to stabilization of the process in both cases. In the case of f = 0.2 mm/rev, the conventional tool exhibits a better stability only at low cutting speeds, while the operation of the LSH tool gets stabilized at high cutting speeds.

ACKNOWLEDGMENTS

The present research was carried out within the pilot project jointly with Siemens Industrial Turbomachinery AB (Sweden) and in part also was supported by the Sustainable Production Initiative (SPI) project.

REFERENCES

Arunachalam, R. and M.A. Mannan (2000) Machinability of nickelbased high temperature alloys. *Machining Sci. Techn.*, **4**, **No.1**, 127-168.

Arunachalam, R.M., Mannan, M.A. and A.C. Spowage (2004) Residual stress and surface roughness when facing age hardened Inconel 718 with CBN and ceramic cutting tools. *Int. J. Machine Tools & Manuf.*, **44**, 879-887.

Bushlya, V., Zhou, J. and J.E. Ståhl (2012) Effect of cutting conditions on machinability of superalloy Inconel 718 during high speed turning with coated and uncoated PCBN tools. *Manufacturing Systems.* 45*th CIRP Conf.*: *Proceed. CIRP*, **3**, 370-375.

Bushlya V., Zhou J., Avdovic P. and J.-E. Ståhl (2013) Wear mechanisms of silicon carbide-whisker-reinforced alumina (Al_2O_3–SiCw) cutting tools when high-speed machining aged Alloy 718. *Int. J. Adv. Manuf. Technol.*, **68**, 1083-1093.

Gotwald, G.A. and I. Melbourne (2009) On the Implementation of the 0-1 Test for Chaos. *SIAM J. Appl. Dynam. Syst*., **8**, 129-145.

Gutnichenko O.A., Bushlya V.M., Zhou J. M., Avdovic P., Simmons U. and J.-E. Ståhl (2013) Dynamic stability of the process of turning nickel superalloys using a toolholder produced by selective laser sintering. *Journal of Superhard Materials*, **35**, **No. 6**, 391-398.

Nakao, W., Ono, M., Lee, S.K., Takahashi, K. and K. Ando (2005) Critical crack healing condition for SiC whisker reinforced alumina under stress. *J. Eur. Ceram. Soc.*, **25**, 3649-3655.

Kumar, A.S., Jiang, W., Brown W.D. and A.P. Malshe (2006) Wear behavior of aluminabased ceramic cutting tools on machining steels. *Tribology International*, **39**, 191-197.

Parka, G., Bement, M.T., Hartman, D.A., Smith, R.E. and Ch.R. Farrar (2007) The use of active materials for machining processes: A review. *Int. J. Mach. Tools Manufact.*, **47**, 2189-2206.

Zhou, J.M., Bushlya, V. and J.-E. Stahl (2012) An investigation of surface damage in the high speed turning of Inconel 718 with use of whisker reinforced ceramic tools. *J. Mater. Proc. Techn.*, **212**, 372-384.

Zhou, J.M., Bushlya, V., Peng, R.L., Johansson, S., Avdovic, P. and J.-E. Stahl (2011) Effects of tool wear on subsurface deformation of nickelbased superalloy. *1st CIRP Conference on Surface Integrity (CSI). Proceed. Engineering*, **19**, 407-413.